pH Modification of Human T-Type Calcium Channel Gating

Brian P. Delisle and Jonathan Satin
Department of Physiology, University of Kentucky College of Medicine, Lexington, Kentucky 40536-0298 USA

ABSTRACT External pH (pH_o) modifies T-type calcium channel gating and permeation properties. The mechanisms of T-type channel modulation by pH remain unclear because native currents are small and are contaminated with L-type calcium currents. Heterologous expression of the human cloned T-type channel, α1H, enables us to determine the effect of changing pH on isolated T-type calcium currents. External acidification from pH_o 8.2 to pH_o 5.5 shifts the midpoint potential ($V_{1/2}$) for steady-state inactivation by 11 mV, shifts the $V_{1/2}$ for maximal activation by 40 mV, and reduces the voltage dependence of channel activation. The α1H reversal potential (E_{rev}) shifts from +49 mV at pH_o 8.2 to +36 mV at pH_o 5.5. The maximal macroscopic conductance (G_{max}) of α1H increases at pH_o 5.5 compared to pH_o 8.2. The E_{rev} and G_{max} data taken together suggest that external protons decrease calcium/monovalent ion relative permeability. In response to a sustained depolarization α1H currents inactivate with a single exponential function. The macroscopic inactivation time constant is a steep function of voltage for potentials < -30 mV at pH_o 8.2. At pH_o 5.5 the voltage dependence of τ_{inact} shifts more depolarized, and is also a more gradual function of voltage. The macroscopic deactivation time constant (τ_{deact}) is a function of voltage at the potentials tested. At pH_o 5.5 the voltage dependence of τ_{deact} is simply transposed by ~40 mV, without a concomitant change in the voltage dependence. Similarly, the delay in recovery from inactivation at V_{rec} of −80 mV in pH_o 5.5 is similar to that with a V_{rec} of −120 mV at pH_o 8.2. We conclude that α1H is uniquely modified by pH_o compared to other calcium channels. Protons do not block α1H current. Rather, a proton-induced change in activation gating accounts for most of the change in current magnitude with acidification.

INTRODUCTION

Voltage-activated calcium channels are critical for regulation of electrical and chemical signaling in the myocardium. Calcium channels are responsible for the generation of action potentials in pacemaker cells and shaping the plateau phase of the cardiac action potential in myocytes. There are two classes of calcium channels expressed in the myocardium, the L- and the T-type calcium channels. These channels differ in their pharmacological, permeation, and gating properties. L-type channels are sensitive to block by dihydropyridines and cadmium, have a greater permeability for barium than calcium, activate at potentials positive to −20 mV, and L-type channel gating regulation is complex (Hille, 1992). L-type channel gating is governed by voltage, calcium, and other intracellular second messengers. In contrast, T-type channels are sensitive to block by nickel (Lee et al., 1999), conduct barium and calcium equally, activate at potentials positive to −70 mV, and their gating is strictly voltage-dependent. The current kinetics of both these channel types are also dramatically different. L-type channels continually reopen in response to depolarization and have a slow decay rate (Hille, 1992). T-type channels open in brief bursts before inactivating. Qualitatively, the T-type channel gating kinetics are sodium channel-like (Droogmans and Nilius, 1989). Both sodium and T-type calcium channel current macroscopic kinetics are well described by the Aldrich, Corey, and Stevens model for sodium channels (Aldrich et al., 1983). However, a major difference between I_{Na} and I_T is that I_T is ~50-fold slower than I_{Na}.

Extracellular acidification commonly accompanies pathophysiological events such as ischemic episodes (reviewed by Carmeliet, 1999). Occlusion of coronary circulation, for example, can change external pH (pH_o) from a normal value of 7.2 to as low as 6.0 (Vanheel et al., 1990; Clark et al., 1993). Extracellular acidification attenuates inward currents measured from both native low-voltage-activated calcium channels (LVA; Tytgat et al., 1990) and high-voltage-activated calcium channels (HVA), including $I_{ca,L}$ (Prod'hom et al., 1987; Krafte and Kass, 1988; Pietrobon et al., 1989). Decreases in calcium current with acidification may be caused by 1) block of the permeation pathway; 2) decrease in local calcium concentrations, and; 3) proton modification of gating. An increase of external proton concentration shifts the voltage dependence of HVA calcium channels gating to more depolarized potentials (e.g., Krafte and Kass, 1988; Kwan and Kass, 1993). This shift effect is similar to that noted for voltage-gated sodium channels (Woodhull, 1973), and T-type calcium channels in cardiac myocytes (Tytgat et al., 1990).

In contrast to L-type calcium channel studies, only scant information exists for regulation of T-type calcium channels. pH_o modulates native I_T differently than L-type channel currents in cardiac myocytes (Tytgat et al., 1990; Cohen et al., 1992). Native myocyte T-currents, however, are difficult to study because myocyte currents are small and hard to isolate. Most native preparations that express I_T also express $I_{Ca,L}$. As a consequence, native I_T is often measured

Received for publication 7 September 1999 and in final form 4 January 2000.

Address reprint requests to Brian P. Delisle, Dept. of Physiology, MS-508, University of Kentucky College of Medicine, Lexington, KY 40536-0298. Tel.: 606-323-1146; Fax: 606-323-1070; E-mail: bpdeli00@pop.uky.edu. or jsatin1@pop.uky.edu.

0006-3495/00/04/1895/11 $2.00

as a subtraction current. Heterologous expression of cloned T-type calcium channels provides a system where I_T can be studied in isolation with native-like kinetics (Satin and Cribbs, 1999). To better understand proton modification of T-type channels, we examined the effect of acidification on the human cardiac T-type channel, α1H (Cribbs et al., 1998), stable-transfected in human embryonic kidney cells (HEK) 293 cells. The major effect of decreasing pH_o on α1H is a shift of steady-state activation gating, with a novel decrease of the voltage dependence of channel activation gating. We also report the unique finding that α1H maximal macroscopic slope conductance increases at pH_o 5.5, compared to 8.2. We conclude that the decrease of inward T-type calcium currents, measured by sustained depolarizations, are mainly due to proton modification of activation gating.

MATERIALS AND METHODS

Cell culture

α1H cDNA (Cribbs et al., 1998) was used to generate a stable-transfected HEK 293 cell line (Satin and Cribbs, 2000). Cells are incubated in DMEM supplemented with 10% fetal bovine serum, 100 U/ml penicillin, 100 mg/ml streptomycin, and 1 mg/ml G-418.

Electrophysiology

Cells were digested with 0.125% trypsin and re-plated 1–3 days before recording in the whole-cell clamp configuration. Culture media were replaced with the extracellular bath solution immediately before recording. The pipette solution contained (in mM): 110 potassium gluconate, 40 CsCl, 1 $MgCl_2$, 5 Mg-ATP, 5 EGTA, 5 Hepes for pH_i 7.4. The extracellular bath solution consisted of (in mM): 140 NaCl, 5CsCl, 2.5 KCl, 10 TEA-Cl, 2.5 $CaCl_2$, 1 $MgCl_2$, 5 glucose, and 5 Hepes for pH_o 8.2–6.8 or 5 MES for pH_o 6.8 to 5.5. The solutions were titrated with CsOH to the appropriate pH. Recordings were initiated 5 min after patch break to allow equilibration of the pipette solution with the cell interior. The cells were recorded in a chamber with a static bath volume of 250 μl. To change pH_o we superfused 6 ml bath solution at 1.5 m/min. Experiments were performed at room temperature (20–22°C). Pipettes were pulled from borosilicate glass to resistance in pipette solution ranging from 1.5 to 2 MΩ. The small spherical cells used for analysis had a mean capacitance of 23 pF $\pm$ 1.2 and we measured a mean series resistance of 4.2 $\pm$ 0.03 MΩ. Currents were filtered at 10 kHZ and sampled at 50 kHz. For voltage steps used in tail current measurements, the capacitative transient was complete in 100–200 μs. All tail current decays are fitted to data after the peak to reduce any complexity introduced by slow settling time of the voltage clamp. Single-exponential functions superimpose the current decay, consistent with a constant $V_{Command}$ during the measurement. pClamp 6.04 and 8.02b programs (Axon Instruments) were used for data analysis and acquisition. Nonlinear curve-fitting was performed with Origins v.4.1 (Microcal Software). Data are reported as mean $\pm$ SEM. Student's *t*-tests on independent groups were used to evaluate *p*-values.

Voltage protocols

Steady-state inactivation is measured by holding at -100 mV, then pre-pulsing from -90 to -30 mV for 5 s, followed by a V_{test} to -20 mV. The peak current of V_{test} is plotted as a function of pre-pulse potential. The data were fit with the Boltzmann distribution:

$$I/I_{max} = (1 - C/1 + \exp(V - V_{1/2})/k) + C \qquad (1)$$

Where I/I_{max} is relative current, V is pre-pulse potential, $V_{1/2}$ is midpoint potential for complete inactivation, k is the slope of the voltage dependence for inactivation, and C is the offset.

Activation gating was measured by holding at -100 followed by a V_{test} from -90 mV to $+40$ mV for 300 ms. The peak current is plotted as a function of V_{test}. We fit the current voltage curves with the Boltzmann form:

$$I(V) = G^*(V - E_{rev})/(1 + \exp(V_{1/2} - V)/k) \qquad (2)$$

Where G is conductance, E_{rev} is the reversal potential, $V_{1/2}$ is the midpoint, and k is the slope of the voltage dependence for maximal inward current. We also measure changes in activation gating by recording tail currents at -80 mV, after pre-pulsing from -85 to $+90$ for 9 ms from a holding potential of -100 mV. The data are fit with a single exponential from cursors set from the peak inward current until the end of the test pulse. Current amplitudes are plotted as a function of pre-pulse potential. The data are fit with Eq. 1.

To assess open channel permeation properties and E_{rev} we pre-pulsed cells from a V_{hold} of -100 mV to $+100$ mV for a duration corresponding to the peak of the outward current (3 ms for pH_o 8.2 and 6 ms for pH_o 8.2; see Results). After the pre-pulse to $+100$ mV we measured current amplitudes at V_{test} ranging from -120 to $+100$ mV (see Fig. 3). E_{rev} was measured from the zero current or by linear extrapolation of voltage steps 5 mV apart.

Deactivation kinetics were determined by holding at -100 mV followed by a $+25$ mV pre-pulse for 20 ms, and then tails were measured by stepping from -40 to -150 mV. The tails were fit with a single exponential to obtain the time constant of current decay (τ_{deact}). τ_{deact} as a function of test potential generates a curve that fits with a single exponential.

Recovery from inactivation is measured by pulsing 5 s to 0 mV followed by a variable recovery interval at V_{rec} -80 or -120 mV. The fraction of recovery current was determined by measuring tails at -80 mV after a 9-ms pre-pulse to $+75$ mV. Tail currents are fit with a single exponential to determine current amplitudes. The data plotted as a function of recovery intervals are fit with a double exponential.

RESULTS

pH_o shifts the voltage dependence of steady-state inactivation

Two parameters define steady-state inactivation of I_T: the midpoint voltage of steady-state availability ($V_{1/2}$), and the slope factor (k), which describes the voltage-dependent availability of this process. External acidification from pH_o 8.2 to 5.5 shifts steady-state inactivation to more depolarized potentials without affecting the slope factor of the steady-state inactivation curve (Fig. 1). Fig. 1, *A* and *B* show the available currents recorded at a V_{test} of -20 mV, after pre-pulsing 5 s from -120 to -30 mV, for pH_o 8.2 and 5.5. At pH_o 5.5 the inward currents are $<$8.2. The decrease of inward current at V_{test} -20 mV is a consequence of a positive shift of activation gating and a change in the voltage dependence of channel activation (see below). The currents are normalized to the maximal inward currents and are plotted as a function of pre-pulse potential. Fig. 1 *C*

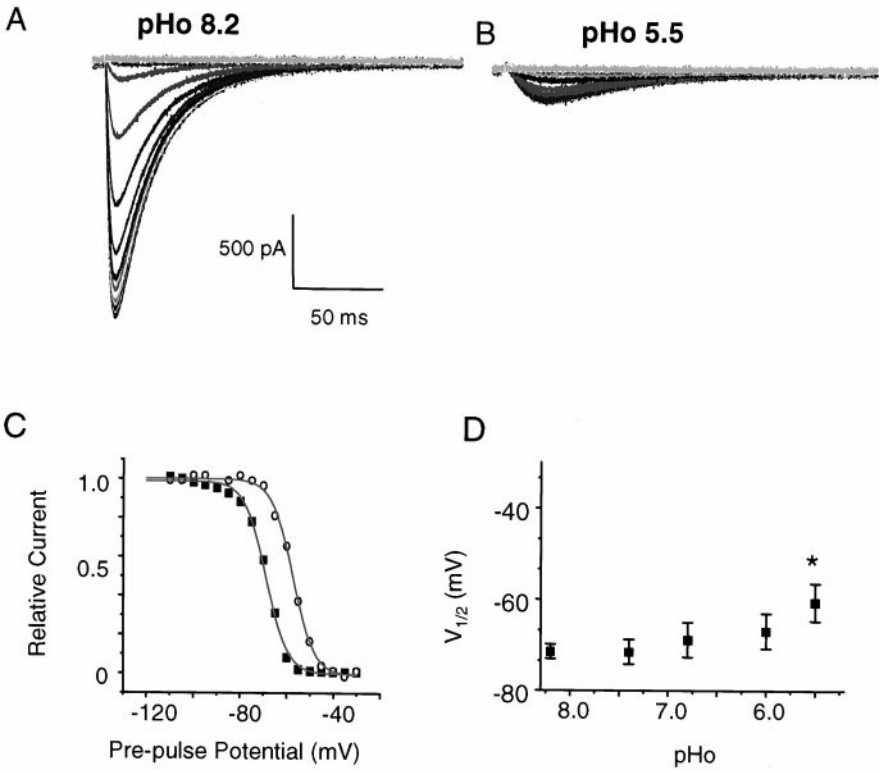

FIGURE 1 External acidification to pH_o 5.5 decreases peak I_T and shifts the voltage dependence of steady-state inactivation. (*A*, *B*) Family of currents for pH_o 8.2 and 5.5 elicited by a V_{test} of −20 mV, following a pre-pulse from −120 to −30 mV for 5 s. (*C*) Peak currents from panels *A* (*squares*), and *B* (*open circles*) are normalized to the peak of the maximally available currents. The relative current is plotted as a function of pre-pulse potential and is fitted with a Boltzmann distribution (*solid line*). The $V_{1/2}$ of inactivation is shifted from −68.7 at pH_o 8.2 to −57.2 at pH_o 5.5, without any effect on the slope (4.6 at pH_o 8.2 and 4.5 at pH_o 5.5). (*D*) A plot of the mean $V_{1/2}$ for inactivation as a function of pH_o shows an 11-mV difference between pH_o 8.2 and 5.5 ($n = 8$; $*p < 0.01$).

shows the change of the relative current plotted as a function of pre-pulse potential from Fig. 1, *A* and *B*. The only effect of changing pH_o from 8.2 to 5.5 is a positive shift of the $V_{1/2}$ by 11 mV ($n = 5$). Fig. 1 *D* summarizes the fitted midpoint as a function of pH_o over the range 8.2–5.5. The only statistically significant shift of $V_{1/2}$ occurs for pH_o 5.5. However, acidification to pH_o 6.0 shifts the mean $V_{1/2}$ by 4 to 5 mV.

pH_o modifies I_T activation voltage dependence and permeation

We used two methods to determine the effects of external acidification on macroscopic I_T activation. First, we measured current-voltage curves from peak inward calcium current by stepping from a V_{hold} of −100 mV followed by a V_{test} ranging from −90 mV to +40 mV for 300 ms. This voltage protocol is restricted to measuring net inward current, and is useful for comparison to data in the literature. Fig. 2 *A* is a plot of the peak inward current plotted as a function of V_{test} for pH_o 8.2 and 5.5 in a representative cell. For this wide pH range the peak inward current decreases, the $I(V)$ curve shifts depolarized, and the voltage dependence decreases. Fig. 2, *B–D* summarize the Boltzmann distribution fit parameters as a function of pH_o ranging from 8.2 to 5.5. Changes in pH_o from 8.2 to 6.8 have no significant effect on conductance, midpoint, or slope of the conductance-transformed $I(V)$ curve. For pH < 6.8 the macroscopic conductance obtained from a linear fit of the ascending limb of the inward $I(V)$ curve begins to decline (Fig. 2 *B*), the $V_{1/2}$ for peak inward current shifts from −51 ± 2 mV (pH_o 8.2) to −17 ± 5 mV (pH_o 5.5; $n = 6$) (Fig. 2 *C*), and the voltage dependence becomes more shallow, changing from 4.6 ± 0.3 mV/*e*-fold at pH_o 8.2 to 8.8 ± 0.6 mV/*e*-fold at pH_o 5.5 ($n = 6$; Fig. 2 *D*).

The potential range tested above may not adequately define changes in the voltage dependence of channel activation and macroscopic conductance. We determined how pH_o modifies both inward and outward currents by stepping from a V_{hold} of −100 to a V_{test} from −90 mV to +100 mV. This extended range peak current-voltage curve shows that peak outward current is greater for pH_o 5.5 than for 8.2 (Fig. 3 *A*). Fig. 3 *B* is the data in panel *A* expanded to show that external acidification causes a hyperpolarizing shift of E_{rev}. The pH_o-induced change in E_{rev} is unequivocal, because at the same potential of +40 mV we measured inward current in pH_o 8.2 and outward current in pH_o 5.5. The reversal potential (E_{rev}) for α1H shifts from 49 ± 1.2 mV at pH_o 8.2 to 36 ± 0.58 mV at pH_o 5.5 ($n = 4$; $p < 0.001$).

The shift of E_{rev} for peak currents elicited by sustained depolarizations suggests a change in selectivity. Therefore, to assess open channel properties we activated channels and measured tail currents elicited by voltage steps to potentials ranging from −120 to +100 mV. The pre-pulse duration was set to the peak of the outward current measured at +100 mV for pH_o 8.2 and 5.5. The open channel current-voltage curve is clearly nonlinear (Fig. 3 *C*). The expanded voltage axis shows unequivocal evidence for a pH_o-induced

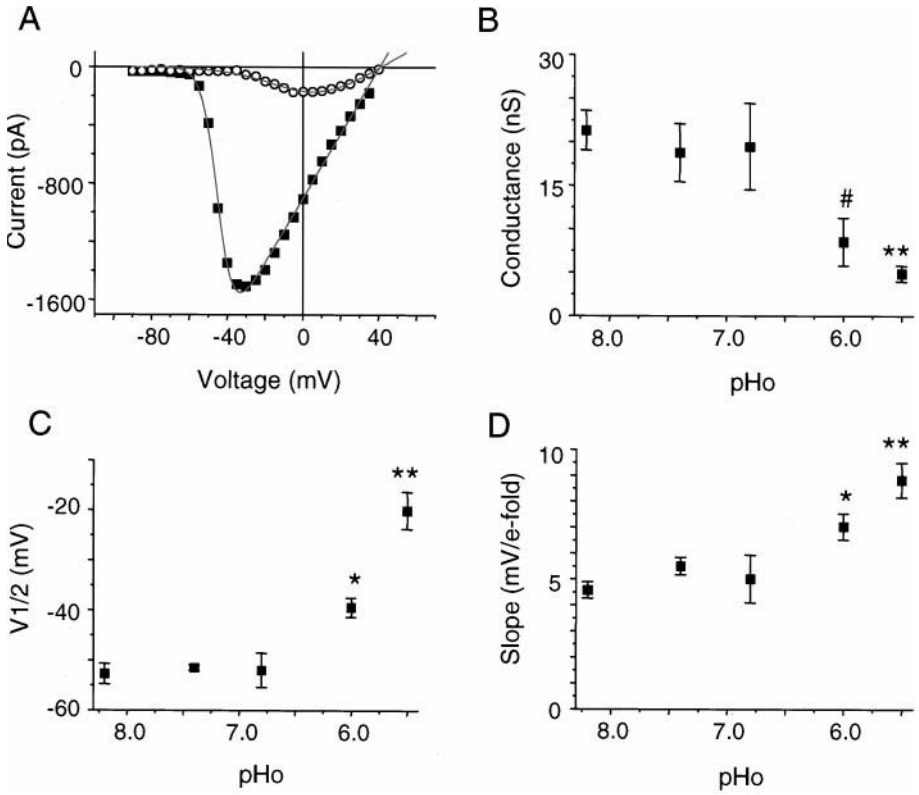

FIGURE 2 External acidification to pH_o 5.5 decreases conductance, shifts the activation $V_{1/2}$ depolarized, and reduces the voltage dependence of activation obtained from the peak $I(V)$ curve. (*A*) Peak inward currents are plotted as a function of V_{test} for pH_o 8.2 (*squares*) and 5.5 (*open circles*) and fitted to a Boltzmann distribution (*solid line*). Acidification from pH_o 8.2 to 5.5 shifts the $V_{1/2}$ for peak current from −45 to −9 mV, decreases the voltage dependence from 4.1 to 8.6 mV/*e*-fold, and decreases conductance from 23 to 5 nS. (*B–D*) The means of the conductance, the midpoint ($V_{1/2}$), and the slope of inward currents derived from the fitted Boltzmann distribution are plotted as a function of pH_o ($n = 14$; $\#p < 0.05$, $*p < 0.01$, $**p < 0.001$).

change in E_{rev} (Fig. 3 *D*). The slope of the open channel current-voltage curve reflects channel conductance. Notice that the maximal slope is in fact slightly steeper for voltages corresponding to inward current at pH_o 5.5 compared to 8.2 (Fig. 3 *C*). The dashed line in Fig. 3 *C* represents the data recorded at pH_o 5.5 shifted by 15 mV, to normalize for the change in E_{rev}. This effect is subtle, but reproducible in all cells tested ($n = 4$, $p < 0.01$). We conclude that acidification increases macroscopic T-type channel slope conductance under our physiological ionic conditions.

External acidification reduces I_T activation voltage dependence

Determining pH effects on I_T activation voltage dependence from the peak inward *I-V* relationship is problematic. To test the effects of external acidification on activation we used a broad range of pre-pulse potentials, followed by a step to a common test potential. We voltage-clamped cells expressing α1H from $V_{hold} = -100$ mV to potentials ranging from −85 to +90 mV for 9 ms, and then measured the instantaneous tail currents elicited by a return step to −80 mV. All tail currents are well-fitted by a single exponential function. This is an important minimal test of adequate voltage control. Fig. 4, *A* and *B* show raw current traces from this tail current voltage protocol at pH_o 8.2 and 5.5. Different prepulse potentials are shown in pH_o 8.2 versus 5.5 because of the dramatic difference in the maximal current activation range for these two conditions (Fig. 4 *C*). In Fig. 4 *A* pre-pulses to −80, −55, −45, −20, and 25 mV are shown. Fig. 4 *B* shows pre-pulses of −80, 0, 25, 70, and 90 mV. Pre-pulses to +75 mV are necessary for maximal current activation at pH_o 5.5 compared to −10 mV for pH_o 8.2. The $V_{1/2}$ for maximal current activation is shifted depolarized and the slope for maximal current activation is about threefold more gradual for pH_o 5.5 than 8.2. Fig. 4, *D* and *E* summarize the pooled data obtained from Boltzmann fits of the tail $I(V)$ curves plotted as a function of pH_o. Acidification from pH_o 8.2 to 5.5 shifts the $V_{1/2}$ for activation by 50 mV. The slope factor is approximately tripled at pHo 5.5 compared to 8.2 (16.0 ± 1.8 and 5.3 ± 1.6 for pH 8.2 and 5.5, respectively).

External acidification shifts and decreases the voltage dependence of τ_{inact}

To characterize the pH_o modification of channel kinetics we measured the effect of pH_o on macroscopic channel inactivation. The decaying phase of current for various sustained depolarizations is well described by a single exponential function for both pH_o 8.2 and 5.5 (Fig. 5, *A* and *B*). The plot of the time constant of inactivation (τ_{inact}) as a function of V_{test} reveals a voltage-dependent and a voltage-independent phase of τ_{inact} for all pH_o tested (Fig. 5 *C*). There is no pH_o-induced change in the voltage-independent τ_{inact} (Fig. 5 *C*, +60 mV). Native I_T can be described by an ACS-like

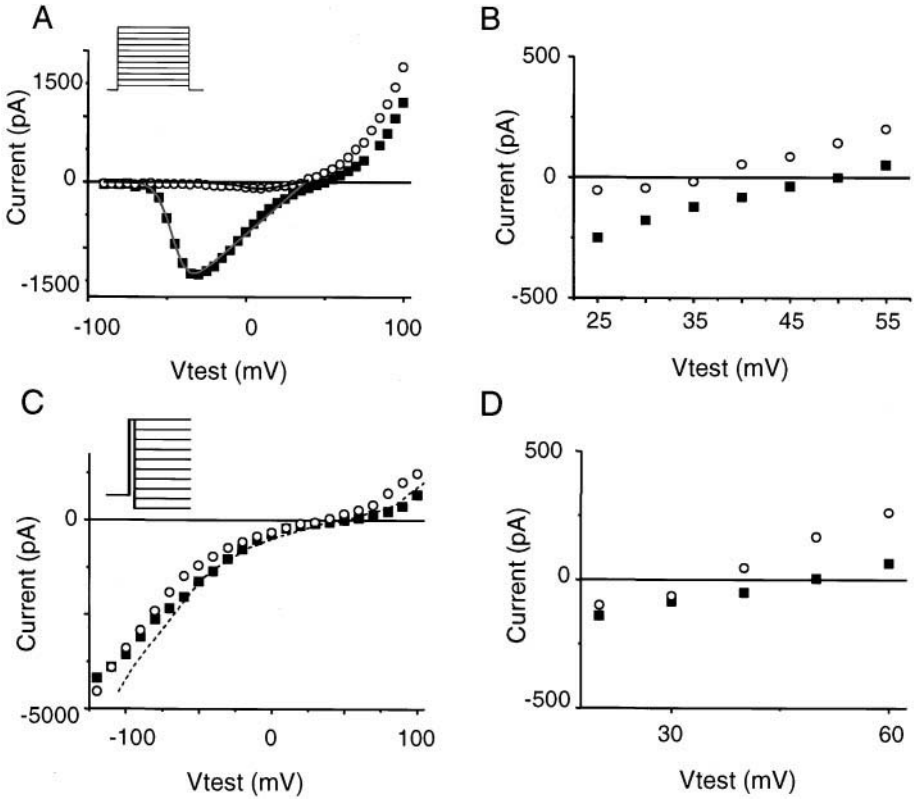

FIGURE 3 External acidification shifts the E_{rev} of α1H I_T and increases macroscopic open channel slope conductance. (*A*) Peak inward current-voltage curve for a representative obtained from a sustained depolarization for pH 8.2 (*solid squares*) and 5.5 (*open circles*). Smooth curve is a modified Boltzmann distribution fit to the inward current as in Fig. 2. (*B*) Same data as in *A*, expanded on voltage axis to show unequivocal demonstration of a change in E_{rev}. Note at +40 mV current is inward for pH 8.2 and outward for 5.5. (*C*) Open channel $I(V)$ curve obtained by pre-pulsing for a duration corresponding to the peak of the current elicited by a +100 mV depolarization. Tail amplitude versus return step potential yields distinctly nonlinear curve. The dashed line was drawn through the data for pH 5.5 (*open circles*) and translated +15 mV to illustrate the increase of slope conductance. (*D*) Same data as in *C*, expanded on voltage axis to show unequivocal demonstration of a change in E_{rev}. Note that at +40 mV current is inward for pH 8.2 and outward for 5.5.

model of gating (Droogmans and Nilius, 1989). A fundamental principle is that for small depolarizations activation is the slow, rate-limiting transition, and therefore contributes to the macroscopic inactivation rate. Following this logic, we predict that acidification should shift and decrease the voltage dependence of the inactivation time constant. Fig. 5 *C* is a plot of the τ_{inact} as a function of voltage for pH_o 8.2 and 5.5. There is not a simple 40–50-mV translation of the $\tau_{inact}(V)$ curve (*dashed line*, Fig. 5 *C*). Consistent with the effects of pH_o modification of steady-state activation gating, the $\tau_{inact}(V)$ is both more gradual and shifted depolarized at pH_o 5.5 relative to 8.2 (Fig. 5 *C*).

External acidification shifts deactivation kinetics on the voltage axis without an effect on voltage dependence

To characterize channel deactivation kinetics we activated channels with a pre-pulse to +25 mV for 20 ms and returned the membrane potential ranging from V_{test} of −40 to −160 mV for pH_o 8.2 and 5.5 (Fig. 6, *A* and *B*). For all V_{test}, and for all pH_o tested the current relaxed with a single exponential (Fig. 6, *C* and *D*). The time constant of deactivation (τ_{deact}) is a function of voltage for the potential range tested. For pH_o 5.5 the voltage-dependence of activation is shifted ~40–50 mV (Figs. 2 and 4). If the deactivation process involves the same voltage-dependent rate transitions as the activation process, but in the opposite net direction, then $\tau_{deact}(V)$ should be altered in response to external acidification. Fig. 6 compares the effect of pH_o 8.2 and 5.5 on the voltage dependence of deactivation. The single-exponential fit the of $\tau_{deact}(V)$ plot (Fig. 6 *E*) yields the slope or voltage dependence of deactivation. Interestingly, the voltage dependence of deactivation (slope = 49 ± 1.2 and 46 ± 1.0 mV/*e*-fold change for pH_o 8.2 and 5.5, respectively) was not significantly affected by pH_o. In fact, a 40-mV shift of $\tau_{deact}(V)$ at pH_o 8.2 superimposes over the $\tau_{deact}(V)$ data at pH_o 5.5 (Fig. 6 *F*). This is in contrast to proton effects on the voltage dependence of activation (Figs. 2 and 4). These data suggest that multiple closed-state transitions of the activation pathway are differentially modified by external pH.

Recovery from inactivation parallels the deactivation response to acidification

In parallel with voltage-gated sodium channels, T-type calcium channels exhibit a delay in recovery from inactivation (Satin and Cribbs, 1999). The delay in the recovery from inactivation is voltage-dependent. This delay is shorter for more hyperpolarized recovery potentials, and becomes negligible at recovery potentials negative to −120 mV. It has been postulated that the delay in recovery from inactivation reflects a voltage-dependent deactivation step necessary for recovery from inactivation (Kuo and Bean, 1994). Because acidification from pH_o 8.2 to 5.5 shifts the $\tau_{deact}(V)$ rela-

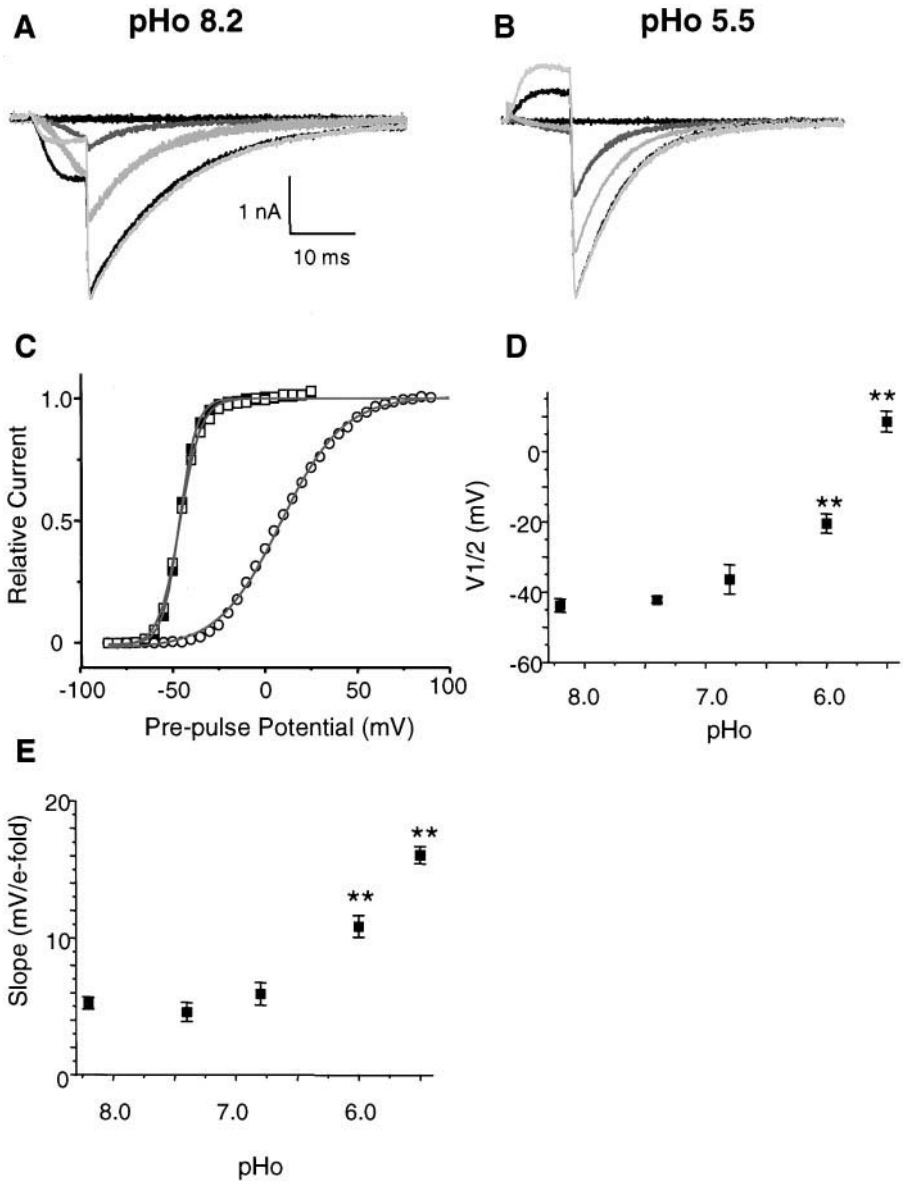

FIGURE 4 External acidification reduces and shifts the voltage dependence for activation. (*A*) pH_o 8.2. Tail currents elicited at a V_{test} of −80 mV after a 9-ms pre-pulse to −80, −55, −45, −20, and 25 mV. (*B*) pH_o 5.5. Tail currents elicited at V_{test} of −80 mV after a 9-ms pre-pulse to −80, 0, 25, 70, and 90 mV. For all pH_o tested the tail current decay is fit by a single exponential. (*C*) The relative tail current amplitudes are plotted as a function of pre-pulse potential for pH_o 8.2 (*squares*), pH_o 5.5 (*open circles*), and washout back to pH_o 8.2 (*open squares*) for a representative cell. The data are fitted with a Boltzmann distribution (*solid line*; $V_{1/2}$ = −46, +9, and −46; k = 4.6, 15.9, and 5.7 for pH_o 8.2, 5.5, and washout with 8.2, respectively). (*D* and *E*) Pooled data from Boltzmann fits from 13 cells. (*D*) External acidification from pH_o 8.2 to 5.5 shifts the $V_{1/2}$ for maximal current activation +50 mV. (**$p < 0.001$) (*E*) Acidification to pH_o 5.5 causes a threefold more shallow slope.

tionship ~40 mV, we wanted to determine whether the voltage dependence of the delay in recovery from inactivation is also shifted by ~40 mV. Recovery from inactivation is measured by pulsing 5 s to 0 mV, followed by a variable recovery interval at recovery potentials (V_{rec}) of −80 or −120 mV. The fraction of recovery current was determined by measuring tail current at −80 mV, following a 9-ms pre-pulse to +75 mV (Fig. 7). We pre-pulsed to +75 mV for 9 ms to maximally activate I_T for pH_o 8.2 and 5.5. Tail currents are fit with a single exponential to determine current amplitudes. The data are normalized to the maximal current recovered at 8 s for each recovery potential. The relative current is plotted as a function of recovery interval (Fig. 7). Fig. 7 *A* shows that there is no significant difference between the fraction of current recovered at V_{rec} = −120 mV for pH_o 8.2 and 5.5. For V_{rec} = −80, the recovery fraction is significantly smaller for recovery intervals <100 ms at pH_o 8.2 compared to pH_o 5.5 (Fig. 7, *B* and *C*). Fig. 7 *D* shows that the fraction of current recovered at pH_o 8.2 and V_{rec} = −120 mV overlaps the fraction of current recovered at pH_o 5.5 and V_{rec} = −80 mV. This result is consistent with a 40-mV shift of deactivation for pH_o 5.5 compared to pH_o 8.2.

DISCUSSION

This study reports the novel finding that external acidification reduces the α1H T-type calcium channel voltage dependence for activation. Similar to most other voltage-dependent cation channels, external acidification causes a reduction of the inward current through α1H. However, this

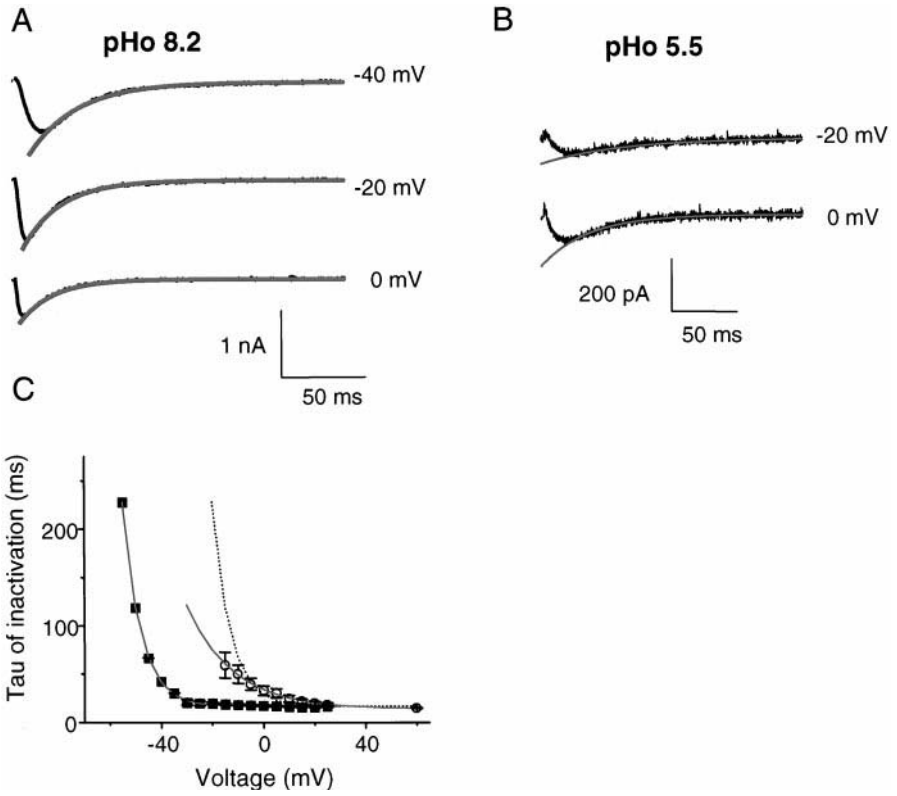

FIGURE 5 External acidification to pH_o 5.5 decreases and shifts the voltage dependence of macroscopic inactivation kinetics. (*A*, *B*) Representative current traces after a sustained depolarization to the V_{test} indicated at pH 8.2 (*A*), or 5.5 (*B*). The time constant of inactivation (τ_{inact}) is obtained by fitting the decay current from the *I*(*V*) protocol with a single exponential (*smooth curve*). (*C*) τ_{inact} is plotted as a function of voltage. At pH_o 8.2 (*squares*) τ_{inact} is voltage independent at potentials positive to −30 mV with an offset of 17 ms. At pH_o 5.5 (*open circles*) τ_{inact} is voltage independent at potentials positive to +55 mV with an offset of 14 ms. Notice the $\tau_{inact}(V)$ curve at pH_o 5.5 shifts more positive and is less voltage dependent than pH_o 8.2 (voltage-dependent slope = 7.0 and 17.8 mV/*e*-fold for pH_o 8.2 and 5.5, respectively). The effect of pH_o on $\tau_{inact}(V)$ is not due to a simple translation on the voltage axis (panel *C*, *dashed line*).

reduction of inward current is only observed for currents elicited by a sustained depolarization. The mechanism underlying this reduction of inward current for the α1H channel is a depolarizing shift and a decrease of the voltage dependence of activation gating.

Paradoxically to the decrease of current elicited by a sustained depolarization, acidification from pH 8.2 to 5.5 actually increases macroscopic slope conductance. External acidification also hyperpolarizing shifts E_{rev}. This is consistent with the postulate that this T-type calcium channel isoform becomes less calcium-selective relative to monovalent ions. It is well established that single calcium channel conductance for monovalent ions is larger than that for divalent cations. Therefore, our data suggest that protonation of the T-type calcium channel simultaneously slows activation gating and reduces calcium selectivity.

External acidification decreases the voltage dependence of activation for α1H

An unexpected major finding of our study was that external protons dramatically reduced the slope factor for the activation curve. To our knowledge there are no reports of proton reduction of voltage dependence in a variety of cation channels that have been extensively studied. This result suggests that T-type channels have evolved unique gating properties. To determine the effect of acidification on activation kinetics we used an isochronal pre-pulse from −85 to +90 mV for 9 ms, followed by a V_{test} to −80 mV. For small depolarizations channel activation is underestimated, because current time-to-peak is >9 ms. The voltage dependence of activation is also obscured by the temporal overlap of inactivation. Nevertheless, an increase in this activation curve slope factor, with acidification, indicates a slowing of the activation rate. These effects are distinct from sodium channel (Woodhull, 1973; Begenisich and Danko, 1983; Daumas and Andersen, 1993; Benitah et al., 1997) or HVA calcium channel modulation by protons in native (Zhou and Jones, 1996) or heterologous expression systems. Both gating charge movement and the energy transferred from the voltage sensor to the gating machinery contribute to this slope factor. Because of the change in slope it is tempting to suggest that external acidification titrates some of the charge involved in voltage sensing, thus reducing the overall gating charge movement. Our conclusion that pH modification involves conformational changes of calcium channels is consistent with the early finding from HVA calcium channels that pH modifies one or more sites on the external surface (Prod'hom et al., 1989).

pH modification of channel kinetics and gating distinguish effects on specific transitions

The change in voltage dependence (slope factor) induced by protons may be separable from the midpoint shift. A number of emerging schemes of T-type channel gating allow us to

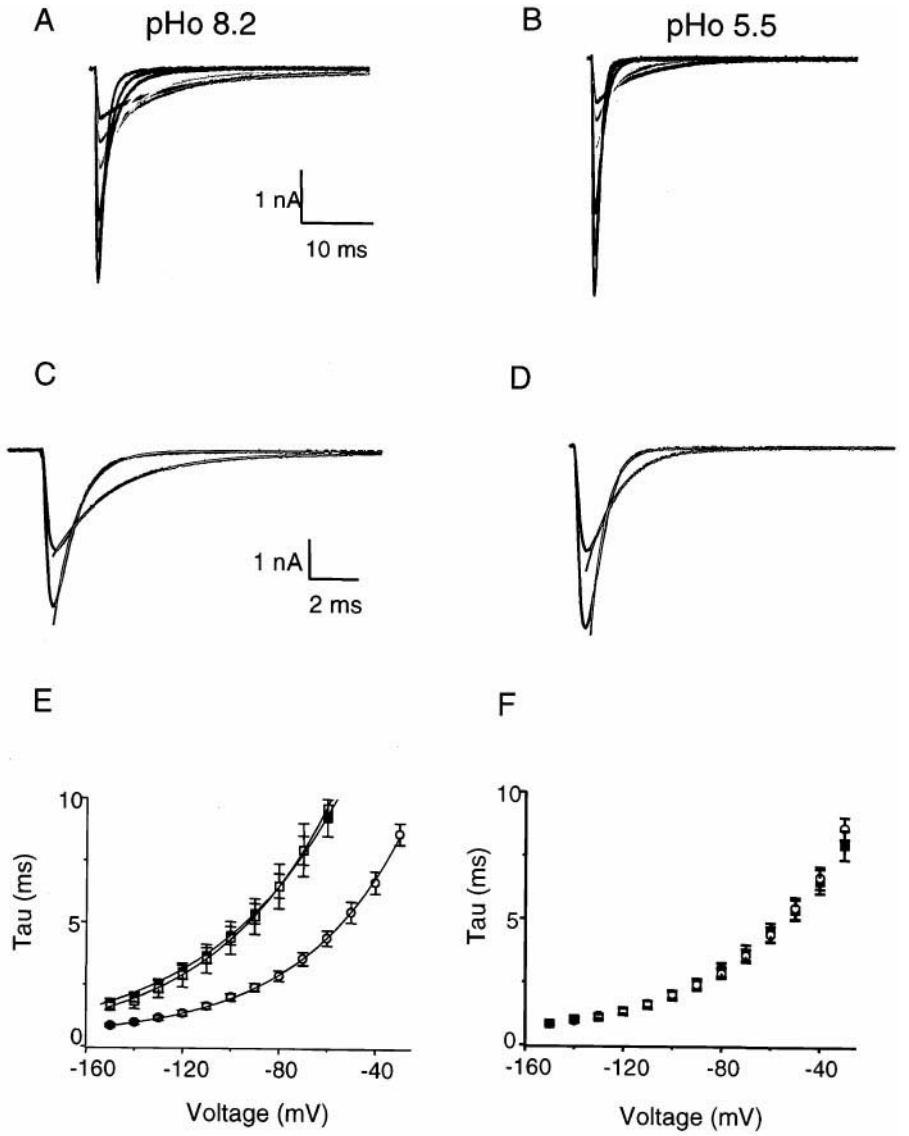

FIGURE 6 In pH_o 5.5 $\tau_{deact}(V)$ shifts +40 mV compared to $\tau_{deact}(V)$ in pH_o 8.2. (*A*, *B*) Tail currents are recorded from a maximally activating potential to V_{test} ranging from −40 to −150 mV. (*C*, *D*) The deactivating tail currents for V_{test} −100 and −150 are well fit with a single exponential (*smooth, solid line*) to obtain the time constant of deactivation (τ_{deact}). (*E*) τ_{deact} is plotted as a function of voltage for pH_o 8.2 (*squares*) and pH_o 5.5 (*open circles*), and is fitted with a single exponential. The slope factor = 49, 46, and 48 does not significantly change for pH_o 8.2, 5.5, and washback to 8.2, respectively. (*F*) The $\tau_{deact}(V)$ data for pH 8.2 shifted by 40 mV and superimposed over the $\tau_{deact}(V)$ data for pH_o 5.5. There is no pH_o effect on the voltage dependence of deactivation.

interpret our shift and voltage-dependent effect with respect to channel state transitions. T-type calcium channels gate with similar features as posed by the ACS model (Aldrich et al., 1983) for a variety of sodium channels. The cloned T-type channels α1G, α1H, and native T-type current share several similar macroscopic kinetic features (Chen and Hess, 1990; Satin and Cribbs, 1999; Serrano et al., 1999). These include voltage-dependent and independent phases of inactivation and deactivation. The voltage-dependent phase of activation can be derived from a slow rate of transfer between closed states at small depolarizations. This would argue that pH effects on steady-state activation should also be reflected in the kinetics of macroscopic inactivation for small depolarizations. This contention is supported by our data.

The voltage-dependent phase of deactivation is dominated by transitions through closed states proximal to the open state. However, in contrast to pH modification of inactivation kinetics, there is only a shift on the voltage axis of the time course of deactivation; pH does not alter the voltage dependence of deactivation. The simplest explanation for these results is that protons slow the voltage dependence of closed transitions distal to opening only. The finding that the proton-induced depolarizing shift is similar for all measures is consistent with a reduction of negative surface potential by protons (Hille et al., 1975). Alternatively, Armstrong and colleagues recently posed the intriguing mechanism that apparent surface potential shifts can in fact be due to intrapore ion binding in sodium channels (Armstrong, 1999; Armstrong and Cota, 1999). The crux of Armstrong's hypothesis is that intrapore calcium in the sodium channel facilitates open-to-close gating of the sodium channel. Lower pH shifts E_{rev} away from E_{Ca}; presumably, this reduces calcium occupancy. Although a surface potential mechanism is consistent with our data, we

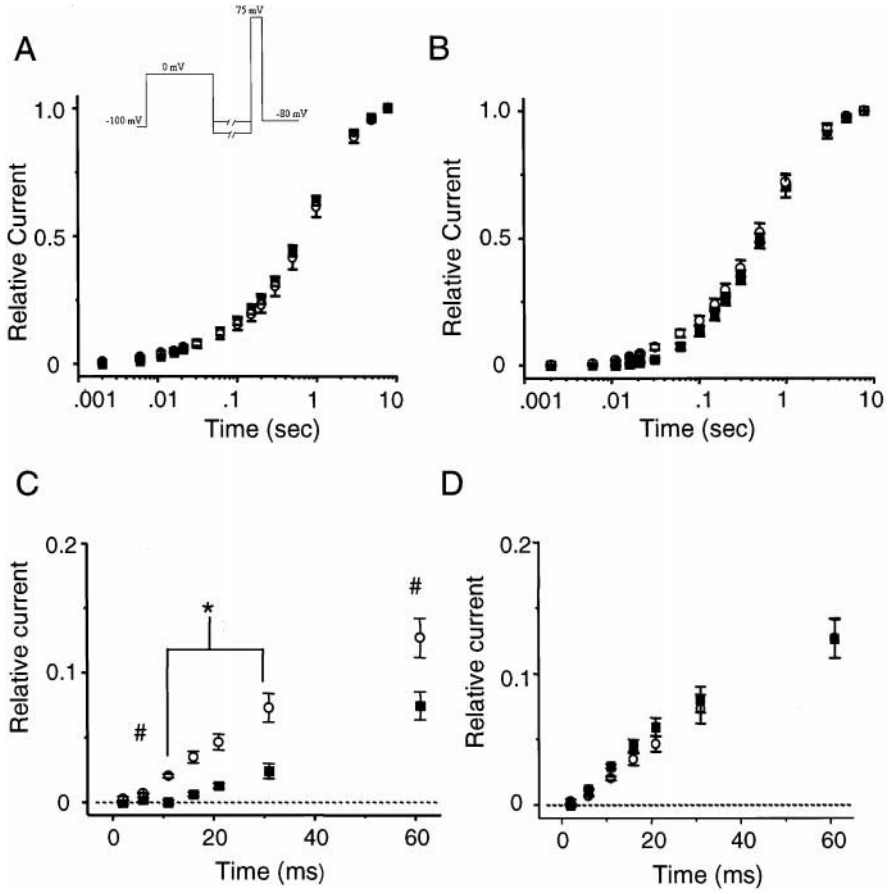

FIGURE 7 The onset of recovery from inactivation at a recovery potential (V_{rec}) of −120 mV and pH_o 8.2 is similar to V_{rec} at −80 mV in pH_o 5.5. Recovery from inactivation is measured by pulsing to 0 mV for 5 s and stepping to −120 or −80 mV for intervals ranging from 0.002 to 8 s (*A*, *inset*). The available currents are measured from tails at −80 mV after stepping to +75 mV for 9 ms. Currents are normalized to the maximal current recovered after 8 s at the test recovery potential. (*A*) The time course of recovery from inactivation for V_{rec} −120 mV for pH_o 8.2 (*squares*) and 5.5 (*open circles*), respectively. There is no significant difference among the data points. (*B*) The time course of recovery from inactivation for V_{rec} −80 mV for pH_o 8.2 (*squares*) and 5.5 (*open circles*). There is no significant difference among the data points at intervals > 60 ms. (*C*) Expanded scale from panel *B* showing the first 60 ms (#$p < 0.05$, *$p < 0.01$). (*D*) At pH_o 5.5 (*open circles*) the recovery of current at V_{rec} −80 mV during the first 60 ms overlaps the recovery of current at pH_o 8.2 (*squares*) and V_{rec} −120 mV.

cannot eliminate a connection between changes in pore properties and channel gating. Future experiments varying ionic conditions are necessary to test whether intrapore ions stabilize individual channel states.

Recovery from inactivation of I_T is distinct from sodium channel recovery in that there is no voltage dependence of the rate of recovery from inactivation (Chen and Hess, 1990; Satin and Cribbs, 1999; Serrano et al., 1999). However, in parallel with sodium channel gating schemes (Kuo and Bean, 1994), there is a voltage dependence to the delay in the onset of recovery from inactivation of I_T (Satin and Cribbs, 1999). The interpretation is that this delay reflects the deactivation through the inactivated states. Our pH modification results are entirely consistent with this scheme for T-type channels. Protons have the same shift effect on voltage dependence of the onset of recovery from inactivation as observed for deactivation.

Native studies of T-type calcium channels suggest that inactivation is linked to channel activation (Droogmans and Nilius, 1989). Therefore, changes in activation gating should be reflected in inactivation gating. The effect on the $V_{1/2}$ for activation is significant at pH_o 6 or less. While we did not find a significant difference in the $V_{1/2}$ for inactivation at pH_o 6.0, there is an ~5 mV mean $V_{1/2}$ depolarizing shift. At pH_o 5.5 this shift achieves statistical significance.

External acidification decreases calcium selectivity and increases inward ionic conductance

The explanation for the increase of maximal macroscopic conductance (G_{max}) is simple in the context of established models of calcium channel selectivity (reviewed by Hille, 1992; also see Deng and McCleskey, 1999). Our experiments were performed in physiological external ionic conditions with respect to calcium and sodium. We show a change in E_{rev} that is consistent with a decrease in relative calcium selectivity (Fig. 3). We also note that the conductance of inward currents is greater at pH_o 5.5 compared to pH_o 8.2. Together, these data suggest that protons are decreasing the affinity of calcium to the pore and increasing monovalent permeation. An increase in monovalent permeation increases conductance, because monovalent ions do not bind to the pore with high affinity (reviewed by Hille, 1992).

Comparison to native cardiac T-type calcium current

There is substantial apparent block by protons of I_T and G_{max} in both native ventricular myocytes (Tytgat et al.,

1990) and atrial cardiac myocytes (Cohen et al., 1992). In the study on ventricular myocytes G_{max} analysis was based on currents elicited by a sustained depolarization (Tytgat et al., 1990; cf., Fig. 1 in our study). Complications with such an interpretation are highlighted in our present study. Although single-channel currents were recorded, the ionic conditions were different. Given our finding that pH modifies selectivity it may be difficult to simply extrapolate single-channel results to macroscopic recordings under mixed ionic conditions. In atrial myocytes (Cohen et al., 1992) the data are qualitatively consistent with our findings with respect to the decrease of slope factor and shift of $V_{1/2}$ in response to protonation. However, atrial T-type channel G_{max} decreases with acidification. In this sole study on atrial myocytes the bath solution contained Ba^{2+} as the charge carrier and no permeant monovalent ions. Therefore, the discrepant decrease of G_{max} from our study may be related to differences in charge carrier. We performed our studies in physiological ionic conditions with respect to sodium and calcium. This simply cannot be done in native tissues because of the overlap of sodium and L-type calcium currents with I_T. In addition, an important limitation of native T-type calcium channel studies is that they rely on subtraction currents. Significant contamination of L-type channels may distort data analysis.

Physiological implications

Although pH_o 5.5 seems extreme, acidification of local external myocardium can reach levels as low as 5.9 after coronary artery occlusion (Axford et al., 1992; Yan and Kleber, 1992). Cardiac hypertrophy is common in patients with ischemic episodes. Native I_T increases in response to hypertrophy (Nuss and Houser, 1993). α1H is a human cardiovascular T-type calcium channel (Cribbs et al., 1998). Therefore, α1H channels may be important pharmacological targets under such pathophysiological conditions. Cardiac hypertrophy and heart failure share the feature of prolonged action potential duration. In both conditions, early after depolarizations (EADs) or spontaneous subthreshold depolarizations (coined SD by Nuss et al., 1999) may generate arrhythmias. While EADs are in part promoted by increased $I_{Ca,L}$ activity (January and Riddle, 1989; Zeng and Rudy, 1995), SDs occur in the subthreshold voltage range where I_T is active (Nuss et al., 1999). The hyperpolarized range of I_T activation is well suited for initiating and sustaining subthreshold oscillatory potentials. There is evidence for this in the myocardium (Hagiwara et al., 1988; Sen and Smith, 1994; Zhou and Lipsius, 1994). If I_T contributes to SD, then local acidification may actually be, in part, protective against abnormal rhythm generation due to attenuation of I_T.

We thank Leanne Cribbs for the α1H clone and for expert advice, Yi Zhang and the UK Cardiovascular Journal Club members for stimulating discussions, and Alison Nemes and Oscar Crawford for technical assistance.

This work was supported in part by a grant from the National Science Foundation.

REFERENCES

Aldrich, R. W., D. P. Corey, and C. F. Stevens. 1983. A reinterpretation of mammalian sodium channel gating based on single channel recording. *Nature.* 306:436–441.

Armstrong, C. M. 1999. Distinguishing surface effects of calcium ion from pore-occupancy effects in Na channels. *Proc. Natl. Acad. Sci. USA.* 96:4158–4163.

Armstrong, C. M., and G. Cota. 1999. Calcium block of Na channels and its effect on closing rate. *Proc. Natl. Acad. Sci. USA.* 96:4154–4157.

Axford, T. C., J. A. Dearani, I. Khait, W. M. Park, M. A. Patel, M. Doursounian, L. Neuringer, C. R. Valeri, and S. F. Khuri. 1992. Electrode-derived myocardial pH measurements reflect intracellular myocardial metabolism assessed by phosphorous 31-nuclear magnetic resonance spectroscopy during normothermic ischemia. *J. Thorac. Cardiovasc. Surg.* 103:902–907.

Begenisich, T., and M. Danko. 1983. Hydrogen ion block of the sodium pore in squid giant axons. *J. Gen. Physiol.* 82:599–618.

Benitah, J. P., J. R. Balser, E. Marban, and G. F. Tomaselli. 1997. Proton inhibition of sodium channels: mechanism of gating shifts and reduced conductance. *J. Membr. Biol.* 155:121–131.

Carbone, E., and H. D. Lux. 1987. Kinetic and selectivity of a low-voltage-activated calcium current in chick and rat sensory neurones. *J. Physiol.* 386:547–570.

Carmeliet, E. 1999. Cardiac ionic currents and acute ischemia: from channels to arrhythmias. *Physiol. Rev.* 79:917–1017.

Chen, C. F., and P. Hess. 1990. Mechanism of gating of T-type calcium channels. *J. Gen. Physiol.* 96:603–630.

Chen, X.-H., and R. W. Tsien. 1997. Aspartate substitutions establish the concerted action of P-region glutamates in repeats I and III in forming the protonation site of L-type Ca channels. *J. Biol. Chem.* 272: 30002–30008.

Clark, K., L. C. Stewart, S. Neubauer, J. A. Balschi, T. W. Smith, J. S. Ingwall, J. F. Nedelac, S. M. Humphrey, A. G. Kleber, and C. S. Springer. 1993. Extracellular volume and transsarcolemmal proton movement during ischemia and reperfusion: a ^{31}P NMR Spectroscopic study of the isovolumic rat heart. *Nmr. Biomed.* 6:278–286.

Coulter, D. A., J. R. Huguenard, and D. A. Prince. 1989. Calcium currents in rat thalamocortical relay neurons: kinetic properties of the transient, low-threshold current. *J. Physiol. (Lond.).* 414:587–604.

Cribbs, L. L., J.-H. Lee, J. Yang, J. Satin, Y. Zhang, A. Daud, J. Barclay, M. P. Williamson, M. Fox, M. Rees, and E. Perez-Reyes. 1998. Cloning and characterization of α1H from human heart, a member of the T-type calcium channel gene family. *Circ. Res.* 83:103–109.

Daumas, P., and O. S. Andersen. 1993. Proton block of rat brain sodium channels: evidence for two proton binding sites and multiple occupancy. *J. Gen. Physiol.* 101:27–43.

Droogmans, G., and B. Nilius. 1989. Kinetic properties of the cardiac T-type calcium channel in the guinea-pig. *J. Physiol.* 419:627–650.

Fox, A. P., M. C. Nowycky, and R. W. Tsien. 1987. Kinetic and pharmacological properties distinguishing three types of calcium currents in chick sensory neurones. *J. Physiol.* 394:149–172.

Hagiwara, N., H. Irisawa, and M. Kameyama. 1988. Contribution of two types of calcium currents to the pacemaker potentials of rabbit sino-atrial node cells. *J. Physiol.* 395:223–253.

Hille, B. 1992. Ionic Channels of Excitable Membranes. 2nd ed., Vols. 3–4. Sinauer Associates, Sunderland, MA.

Hille, B., A. M. Woodhull, and B. I. Shapiro. 1975. Negative surface charge near sodium channels of nerve: divalent ions, monovalent ions, and pH. *Philos. Trans. R. Soc. Lond. B.* 270:301–318.

January, C. T., and J. M. Riddle. 1989. Early afterdepolarizations: mechanism of induction and block. A role for L-type Ca^{++} current. *Circ. Res.* 64:977–990.

Klockner, U., G. Mikala, A. Schwartz, and G. Varadi. 1996. Molecular studies of the asymmetric pore structure of the human cardiac voltage-dependent calcium channel. *J. Biol. Chem.* 271:22293–22296.

Krafte, D. S., and R. S. Kass. 1988. Hydrogen ion modulation of Ca channel current in cardiac ventricular cells. Evidence for multiple mechanisms. *J. Gen. Physiol.* 91:641–657.

Kuo, C.-C., and B. P. Bean. 1994. Na^+ channels must deactivate to recover from inactivation. *Neuron.* 12:819–829.

Kwan, Y. W., and R. S. Kass. 1993. Interactions between protons and calcium near L-type calcium channels: evidence for independent channel-associated binding sites. *Biophys. J.* 65:1188–1195.

Lee, J-H., J. C. Gomora, L. L. Cribbs, and E. Perez-Reyes. 1999. Nickel block of three cloned T-type calcium channels: low concentrations selectively block α1H. *Biophys. J.* 77:3034–3042.

Nuss, H. B., and S. R. Houser. 1993. T-type Ca^{2+} current is expressed in hypertrophied adult feline left ventricular myocytes. *Circ. Res.* 73: 777–782.

Nuss, H. B., S. Kaab, D. A. Kass, G. F. Tomaselli, and E. Marban. 1999. Cellular basis of ventricular arrhythmias and abnormal automaticity in heart failure. *Am. J. Physiol. Heart Circ. Physiol.* 277:H80–H91.

Pietrobon, D., B. Prod'hom, and P. Hess. 1989. Interactions of protons with single open L-type calcium channels. *J. Gen. Physiol.* 94:1–21.

Prod'hom, B., D. Pietrobon, and P. Hess. 1987. Direct measurement of proton transfer rates to a group controlling the dihydropyridine-sensitive calcium channel. *Nature.* 329:243–246.

Prod'hom, B., D. Pietrobon, and P. Hess. 1989. Interactions of protons with single open L-type calcium channels. Location of protonation site and dependence of proton-induced current fluctuations on concentration and species of permeant ion. *J. Gen. Physiol.* 94:23–42.

Satin, J., and L. L. Cribbs. 1999. Molecular identification and functional characterization of a splice variant of T-type calcium channel in atrial myocytes. *Circ.* 100:abstract.

Satin, J., and L. L. Cribbs. 2000. Identification of a T-type calcium channel in murine atrial myocytes (AT-1 cells). *Circ. Res.* 86:(in press).

Sen, L., and T. W. Smith. 1994. T-type Ca^{2+} channels are abnormal in genetically determined cardiomyopathic hamster hearts. *Circ. Res.* 75: 149–155.

Serrano, J. R., E. Perez-Reyes, and S. W. Jones. 1999. State-dependent inactivation of the α1G T-type calcium channel. *J. Gen. Physiol.* 114: 185–201.

Tombough, G. C., and G. G. Somjen. 1996. Effects of extracellular pH on voltage gated Na, K, and Ca currents in isolated rat CA1 neurons. *J. Physiol.* 493:719–732.

Tytgat, J., B. Nilius, and E. Carmeliet. 1990. Modulation of the T-type cardiac Ca channel by changes in proton concentration. *J. Gen. Physiol.* 96:973–990.

Vanheel, B., A. DeHemptinne, and I. Leusen. 1990. Acidification and intracellular sodium ion activity during simulated myocardial ischemia. *Am. J. Physiol. Cell Physiol.* 259:C169–C179.

Woodhull, A. M. 1973. Ionic blockage of sodium channels in nerve. *J. Gen. Physiol.* 61:687–708.

Yan, G. X., and A. G. Kleber. 1992. Changes in extracellular and intracellular pH in ischemic papillary muscle. *Circ. Res.* 271:460–470.

Zeng, J., and Y. Rudy. 1995. Early after-depolarizations in cardiac myocytes: mechanism and rate dependence. *Biophys. J.* 68:949–964.

Zhou, W., and S. Jones. 1996. The effects of external pH on calcium channel currents in bullfrog sympathetic neurons. *Biophys. J.* 70: 1326–1334.

Zhou, Z., and S. L. Lipsius. 1994. T-type calcium current in latent pacemaker cells isolated from cat right atrium. *J. Mol. Cell. Cardiol.* 26: 1211–1219.